# Supplementary Material for "Repetitive small seismicity coupled with rainfall can trigger large slope instabilities on metastable volcanic edifices"

Durand Virginie<sup>1,2\*</sup>, Mangeney Anne<sup>2</sup>, Bernard Pascal<sup>2</sup>, Jia Xiaoping<sup>3</sup>, Bonilla Fabian<sup>2,4</sup>, Satriano Claudio<sup>2</sup>, Saurel Jean-Marie<sup>2</sup>, Aissaoui El Madani<sup>2</sup>, Peltier Aline<sup>2,5</sup>, Ferrazzini Valérie<sup>2,5</sup>, Kowalski Philippe<sup>2,5</sup>, Lauret Frédéric<sup>2,5</sup>, Brunet Christophe<sup>2,5</sup> and Hibert Clément<sup>6</sup>

<sup>1</sup>Université Côte d'Azur, IRD, CNRS, Observatoire de la Côte d'Azur, Géoazur, Sophia-Antipolis, France.

<sup>2</sup>Université de Paris, Institut de Physique du Globe de Paris, CNRS, Paris, F-75005, France.

<sup>3</sup>Institut Langevin, ESPCI Paris Tech, CNRS UMR 7587, Paris, France.

<sup>4</sup>Geotechnical Engineering, Environment, Natural Hazards and Earth Sciences Department, Université Gustave Eiffel, Marne-la-Vallée, 77447, France.

<sup>5</sup>Observatoir Volcanologique du Piton de la Fournaise, Institut de Physique du Globe de Paris, La Plaine des Cafres, F-97418, La Réunion, France.

<sup>6</sup>Institut Terre Environnement de Strasbourg, ITES, CNRS UMR 7063, University of Strasbourg/EOST, Strasbourg, France.

\*Corresponding author(s). E-mail(s): virginie.durand@geoazur.unice.fr;

### 2

# This PDF file includes:

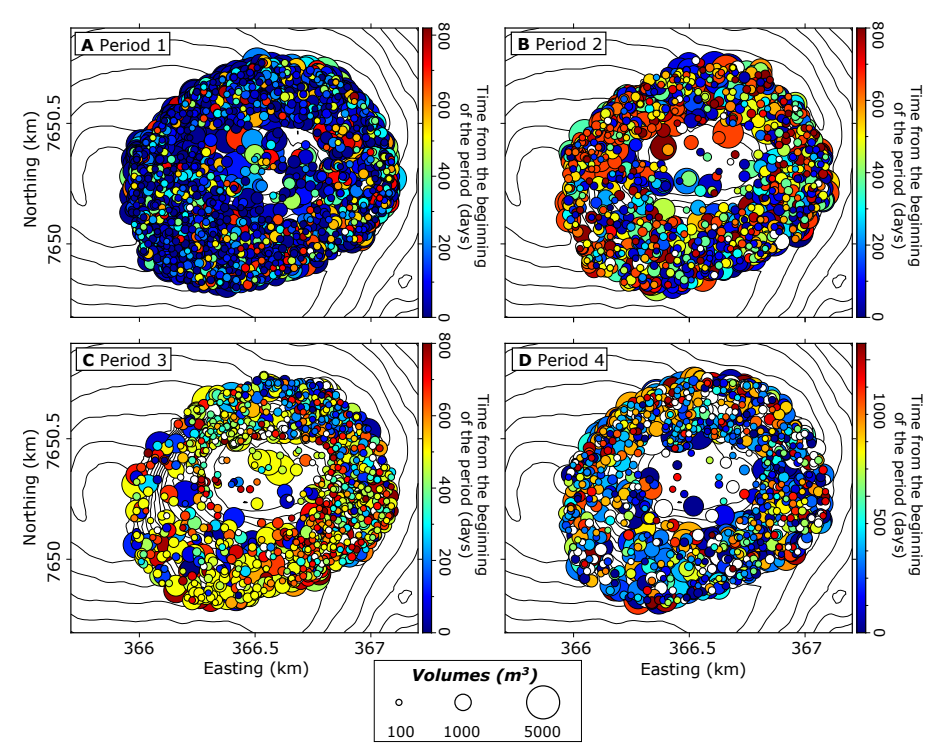
- Supplementary Methods. Description of the methods used to differentiate the impact of seismicity (VTs) and deformation on rockfall triggering.
- Supplementary Figure S1. Spatio-temporal evolution of the smallest rockfalls  $(V \le 5000m^3).$
- Supplementary Figure S2. Comparison of rockfall activity to volcanotectonic events (VTs) and rainfall at the summit of the Piton de la Fournaise volcano for the whole rockfall catalog.
- Supplementary Figure S3. Significance of the observations of triggering by seismicity and rainfall for the whole rockfall catalog.
- Supplementary Figure S4. Illustration of the declustering of the rockfall catalog.
- Supplementary Figure S5. Gamma-distributions.
- Supplementary Figure S6. Significance of the observations of triggering by seismicity and rainfall for the declustered rockfall catalog.
- Supplementary Figure S7. Comparison of rockfall activity to volcanotectonic events (VTs) and rainfall at the summit of the Piton de la Fournaise volcano for rockfalls with volume greater than  $1000m^3$ .
- Supplementary Figure S8. Comparison of rockfall activity to volcanotectonic events (VTs) and rainfall at the summit of the Piton de la Fournaise volcano for rockfalls with volume smaller than  $5000m^3$ .
- Supplementary Figure S9. Comparison of rockfall activity and seismic moment of volcano-tectonic events.
- Supplementary Figure S10. Comparison of the temporal evolution of the rockfalls and of the deflation and inflation of the volcano cone.
- Supplementary Figure S11. Statistical tests to differentiate the impact of seismicity (VTs) and deformation on rockfall triggering.
- Supplementary Figure S12. Spatio-temporal evolution of the rockfalls during the 2013 crisis (2013/02/01-2013/06/13).
- Supplementary Figure S13. Schematic representation of the different mechanisms driving rockfalls during Periods 1 and 2.

# Supplementary Methods:

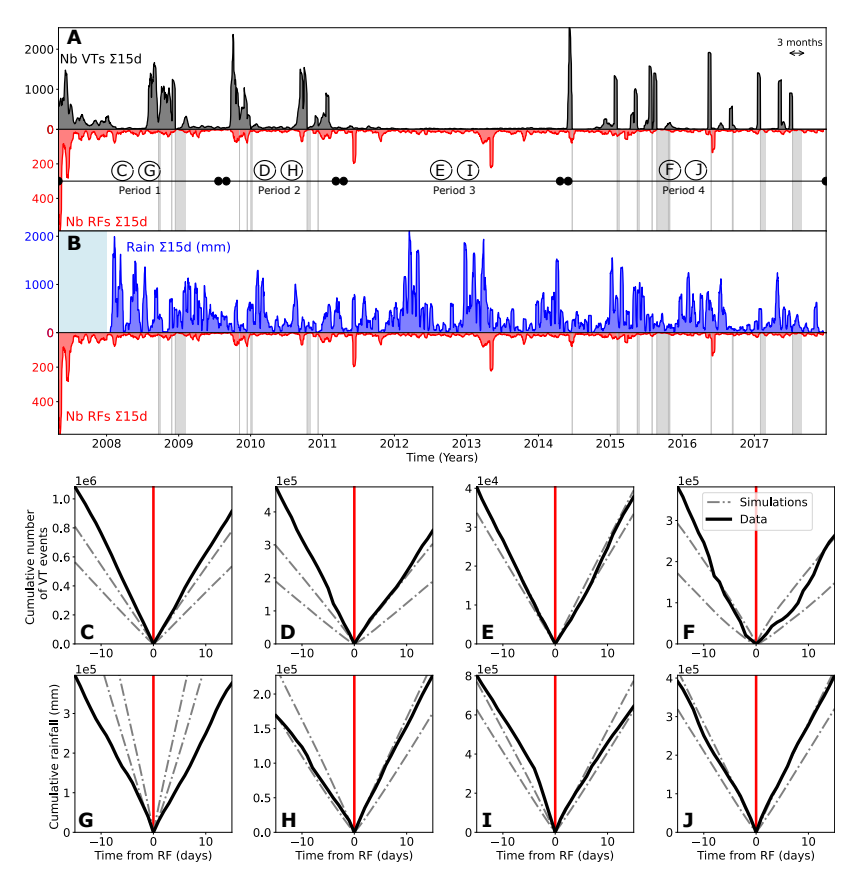
The slopes are also exposed to the global deformation of the summit measured by GNSS stations (Fig. 2C). This deformation and seismic activity are linked to the magma pressurization and circulation at depth before eruptions and therefore generally occur simultaneously. Consequently, with these data, it is difficult to differentiate their exact role in the triggering of rockfalls. The seismicity generates repetitive and dynamic ground shaking. It has been shown, especially for earthquake triggering, that this dynamic ground shaking can trigger a rupture on the short-term, through dynamic damage processes. On the other hand, the deformation of the summit is small and slow ( 10 cm over 1 km in more than one day, i.e. a strain rate of 10-9/s). This can increase the static forcing due to gravity that is applied on the slopes, bringing them closer to failure, but not likely triggering rockfalls on the short-term, as the cumulative tilt angle remains very small (less than 1°). However, the large summit deformation due to inflation and deflation cycles of the volcano between the eruptions may also expand the fractures and damage zones, thus bringing the slopes closer to failure on the long-term.

In order to investigate their relative influence on rockfall triggering, we separate days exhibiting deflation from those exhibiting inflation. The quasiconstant deflation rates of the summit appear to have no influence on rockfall activity, as illustrated in Fig. S5. However, some jumps in inflation occur before rockfall episodes. To separate more robustly the influence of the inflation rate from the influence of the seismicity, we compute the median of the daily rate of volcano-tectonic events and the median of the inflation rate distributions over different periods. We perform statistical tests considering only the days where the seismic activity is dominant (i.e. when the number of events per day is greater than the median seismicity rate and the inflation rate is lower than the median of deformation rate) and the days where the inflation rate is dominant (i.e. when the number of events per day is lower than the median seismicity rate and the inflation rate is greater than the median of the deformation rate). These tests show that during times where the deformation is low (left column in Fig. S6), the influence of seismicity on the rockfall rate is clear (Fig. S6 B and D), whereas when the seismicity is low (right column in Fig. S6), no clear effect of the deformation on the rockfall rate is visible. This suggests that changes in the inflation rate are not a direct triggering factor for rockfalls.

# 4 Article Title

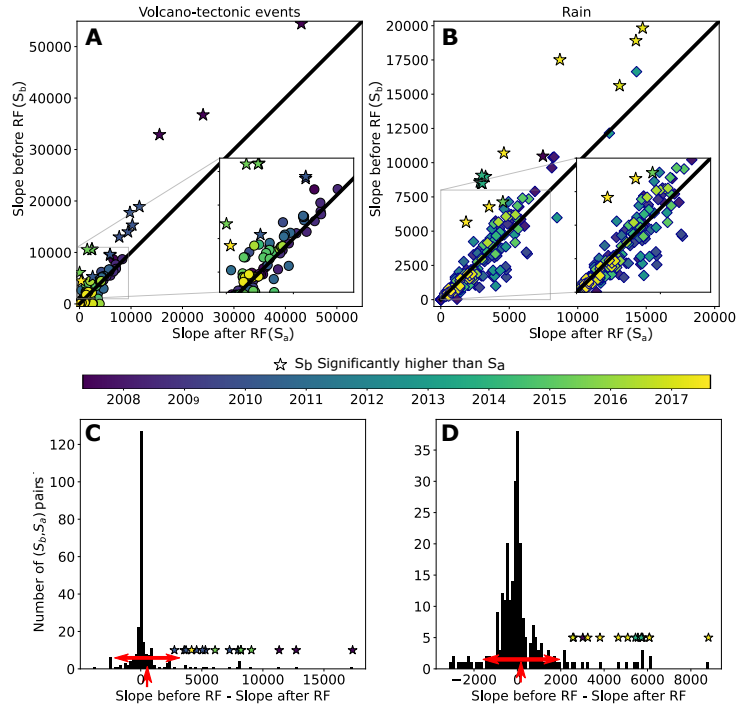


Supplementary Figure S1 Spatio-temporal evolution of the smallest rockfalls ( $V \leq 5000m^3$ ). The size of the circles scales with the volumes of the rockfalls, the colors represent the time from the beginning of each period. The smallest rockfalls are homogeneously distributed on the crater walls, for each period.

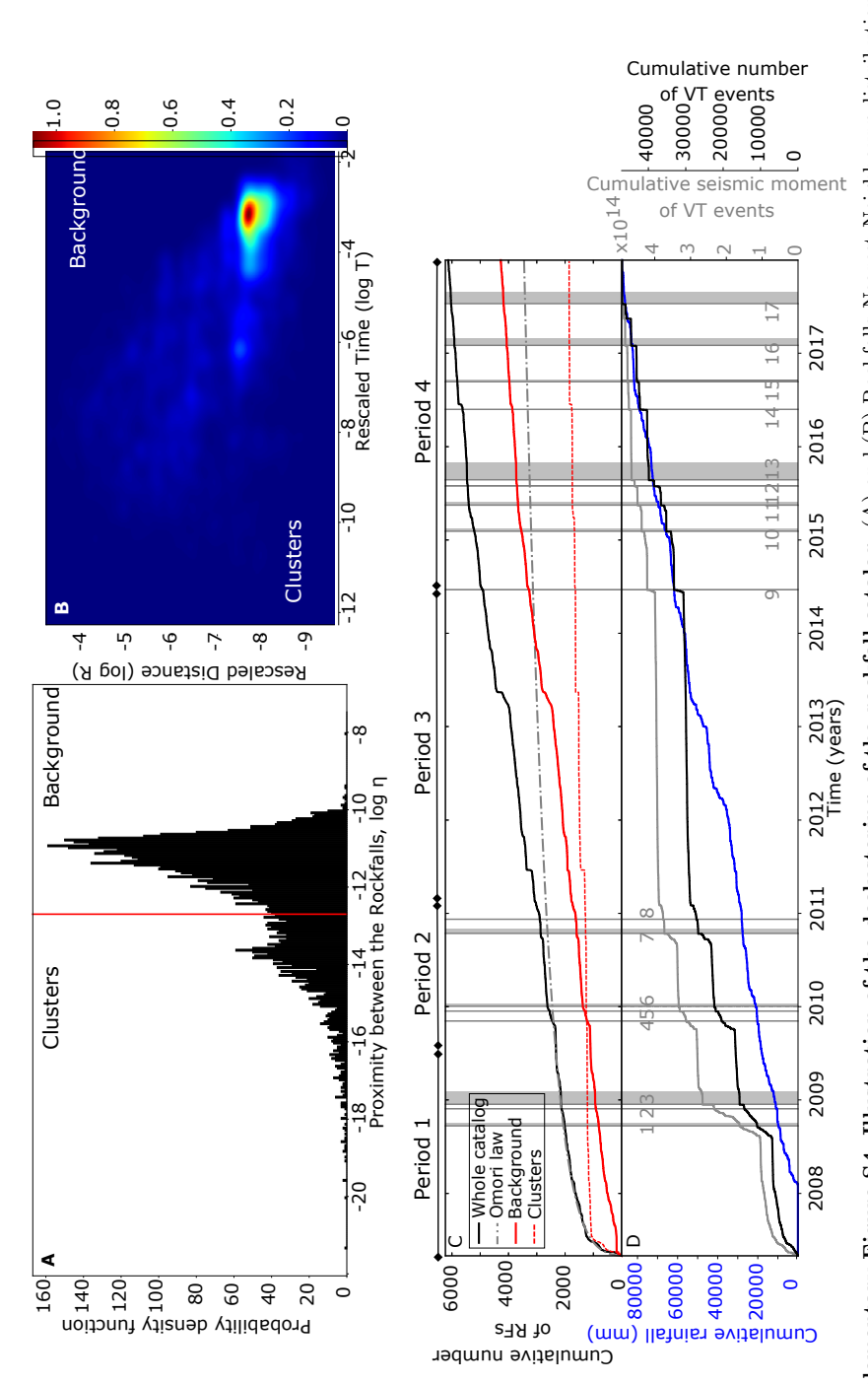


Supplementary Figure S2 Comparison of rockfall activity to volcano seismicity and rainfall at the summit of the Piton de la Fournaise Volcano for the whole rockfall catalog. (A) Number of volcano-tectonic events (VT, black) vs. the number of rockfalls (RF, red), both summed over 15 days. The vertical gray lines and rectangles show the start times and durations of eruptions. The horizontal black lines delimited by dots mark the different time spans used in (C) to (J). (B) Rainfall amount (blue) vs. the number of rockfalls (red), both summed over 15 days. The light blue rectangle indicates the period over which no rain data is available. (C) to (F) Statistical significance of the effect of seismicity on rockfall triggering. The plots are centered around the time of the rockfall occurrence (red vertical line). The dashed gray lines show the 95% confidence intervals for the simulations, i.e. the zones where the link between seismicity and rockfall occurrences is not significant. The black lines represent the seismicity data stacked for all rockfalls. The periods used for each plot are indicated on (A). For more details on how these plots are made, see Materials and Methods. (G) to (J) Same as (C) to (F), for rainfall.

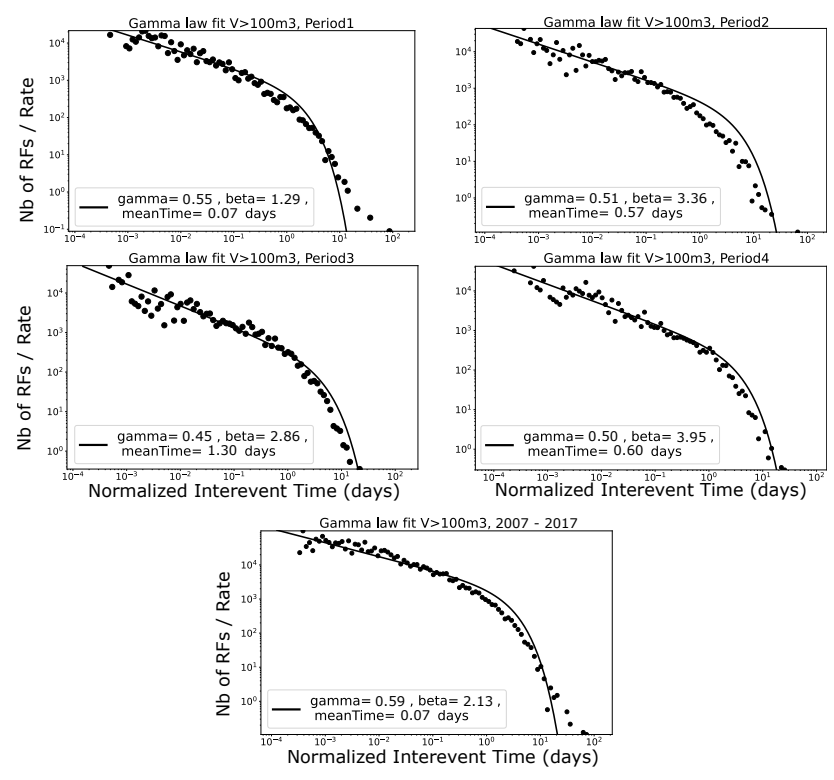
# Article Title



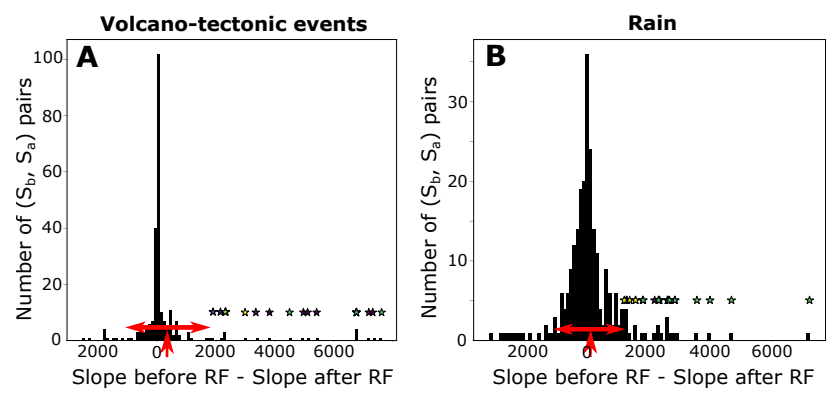
Supplementary Figure S3 Significance of the observations of triggering by seismicity and rainfall for the whole rockfall catalog. (A) Slope of the stacked seismicity before  $(S_b)$  vs. after  $(S_a)$  the rockfalls. The black line is where the two slopes are equal (i.e. same cumulative number of volcano-tectonic events before and after the rockfalls). The slopes are computed on stacked data in 4-month long moving windows, each shifted by 15 days from the previous one. The stars show when the slope before the rockfalls is significantly larger than the slope after. The dots and stars are color-coded to show time. (B) Same as (A) for rainfall. See Materials and Methods for more details on the computation of the slopes. (C) and (D) Distributions of the slope differences for seismicity and rainfall respectively. The vertical red arrows indicate the mean values of the distributions and the horizontal red arrows indicate the  $+/-\sigma$  range. The stars are the same as for (A) and (B).



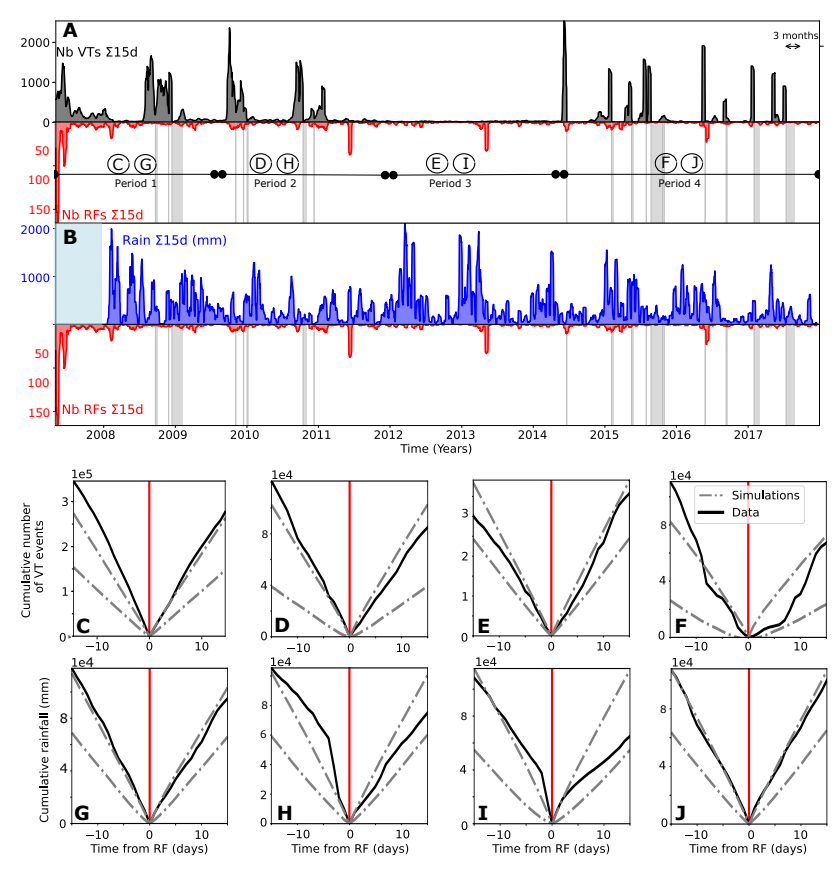
(B) Joint distribution of rescaled time (T) and space (R) components. The white line logR + logT = -12.7 is the equivalent of the red one of figure (A). (C) Cumulative number of events for the background activity (continuous red line) and for the clustered events (dashed red line), compared to the whole catalog (continuous black line) and the Omori fit (dashed gray line). (D) Temporal evolution of rainfall (blue) and shallow volcano-tectonic (A) Histogram of the nearest-neighbor distance  $\eta$ . The threshold distance (red line)  $log\eta = -12.7$  separates the background and clusters activities. Supplementary Figure S4 Illustration of the declustering of the rockfall catalog. (A) and (B) Rockfalls Nearest-Neighbourg distribution. (VT) events plotted as cumulative number (black) and cumulative seismic moment (gray).



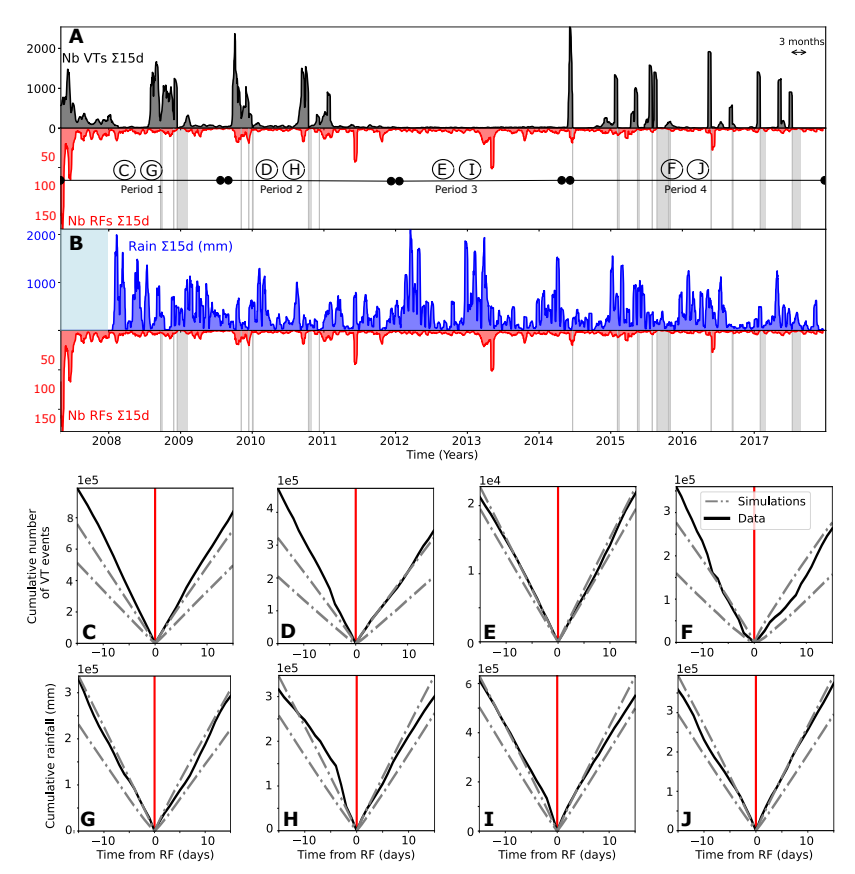
Supplementary Figure S5 Interevent time distribution per period. The gamma law fits showed on this figure are the ones used to generated the synthetic catalogs. Periods are the same as for Fig. S1. The periods used for each plot are indicated on Fig. 3A and 4 in the main text. The bottom figure shows the gamma law fit for the whole period (2007-2017). The parameters for this fit are used in the analysis of Figures 6C and D.



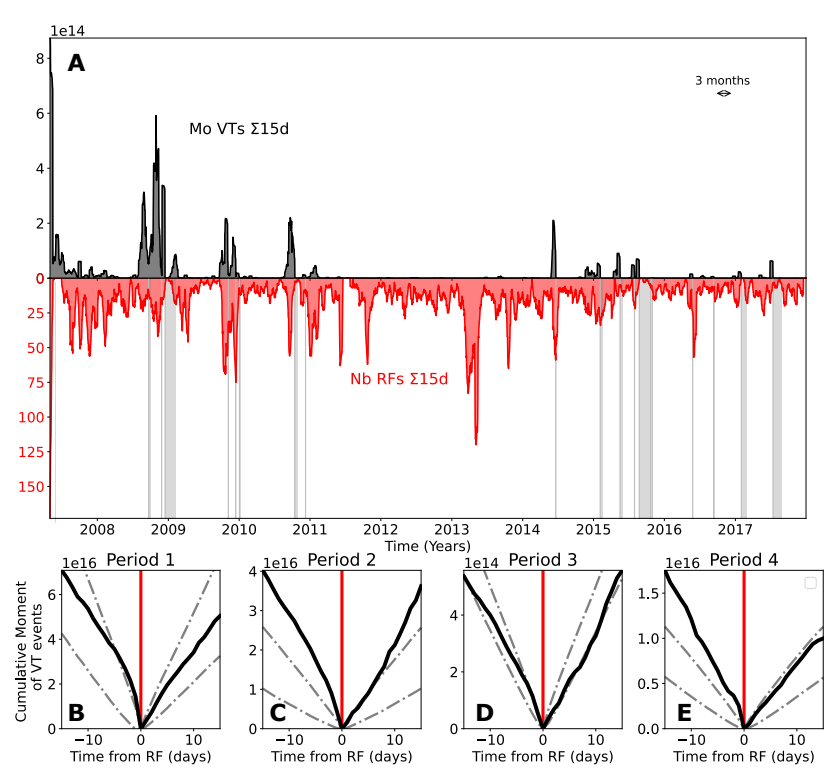
Supplementary Figure S6 Significance of the observations of triggering by seismicity and rainfall for the declustered rockfall catalog. (A) and (B) Distributions of the slope differences for seismicity and rainfall respectively. The vertical red arrows indicate the mean values of the distributions and the horizontal red arrows indicate the  $+/-\sigma$  range. The stars are the same as for Figures 6A and B. Figures S3 A and B show an asymmetry in the distribution of the rate differences  $R_b - R_a$ , with abnormally high  $R_b - R_a$  values. For the seismicity, we find a probability of 0.02% that these high  $R_b - R_a$  values occur by chance. This clearly shows that a significant portion of the rockfalls are triggered by seismicity. The rockfalls showing the highest relative differences  $R_b - R_a$ , indicated by stars in Figures ??, and causing the asymmetry of the distribution, are thus very likely to be triggered by seismicity. For the rain, we find a probability of 3.9% that high  $R_b - R_a$  values occur by chance. This means that rainfall has a probable impact on rockfall triggering, although less significant than the impact of seismicity.



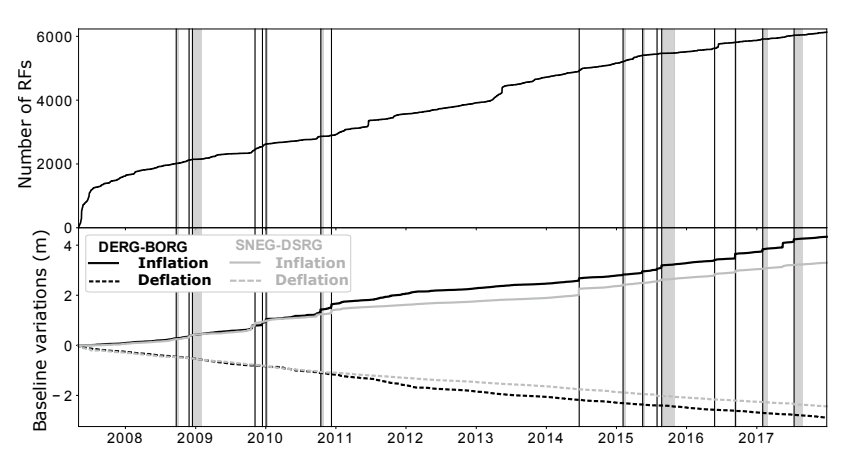
Supplementary Figure S7 Comparison of rockfall activity to volcano-tectonic events (VTs) and rainfall at the summit of the Piton de la Fournaise volcano for rockfalls with volume greater than  $1000m^3$ . The catalog used in this figure is the non-declustered one. (A) Number of volcano-tectonic events (VT, black) vs. the number of rockfalls (RF, red), both summed over 15 days. The vertical gray lines and rectangles show the start times and durations of eruptions. The horizontal black lines delimited by dots mark the different time spans used in (C) to (J). (B) Rainfall amount (blue) vs. the number of rockfalls (red), both summed over 15 days. The light blue rectangle indicates the period over which no rain data is available. (C) to (F) Statistical significance of the effect of seismicity on rockfall triggering. The plots are centered around the time of the rockfall occurrence (red vertical line). The dashed gray lines show the 95% confidence intervals for the simulations, i.e. the zones where the link between seismicity and rockfall occurrences is not significant. The black lines represent the seismicity data stacked for all rockfalls. The periods used for each plot are indicated on (A). For more details on how these plots are made, see Materials and Methods. (G) to (J) Same as (C) to (F), for rainfall.



Supplementary Figure S8 Comparison of rockfall activity to volcano-tectonic events (VTs) and rainfall at the summit of the Piton de la Fournaise volcano for rockfalls with volume smaller than  $5000m^3$ . The catalog used in this figure is the non-declustered one. (A) Number of volcano-tectonic events (VT, black) vs. the number of rockfalls (RF, red), both summed over 15 days. The vertical gray lines and rectangles show the start times and durations of eruptions. The horizontal black lines delimited by dots mark the different time spans used in (C) to (J). (B) Rainfall amount (blue) vs. the number of rockfalls (red), both summed over 15 days. The light blue rectangle indicates the period over which no rain data is available. (C) to (F) Statistical significance of the effect of seismicity on rockfall triggering. The plots are centered around the time of the rockfall occurrence (red vertical line). The dashed gray lines show the 95% confidence intervals for the simulations, i.e. the zones where the link between seismicity and rockfall occurrences is not significant. The black lines represent the seismicity data stacked for all rockfalls. The periods used for each plot are indicated on (A). For more details on how these plots are made, see Materials and Methods. (G) to (J) Same as (C) to (F), for rainfall.

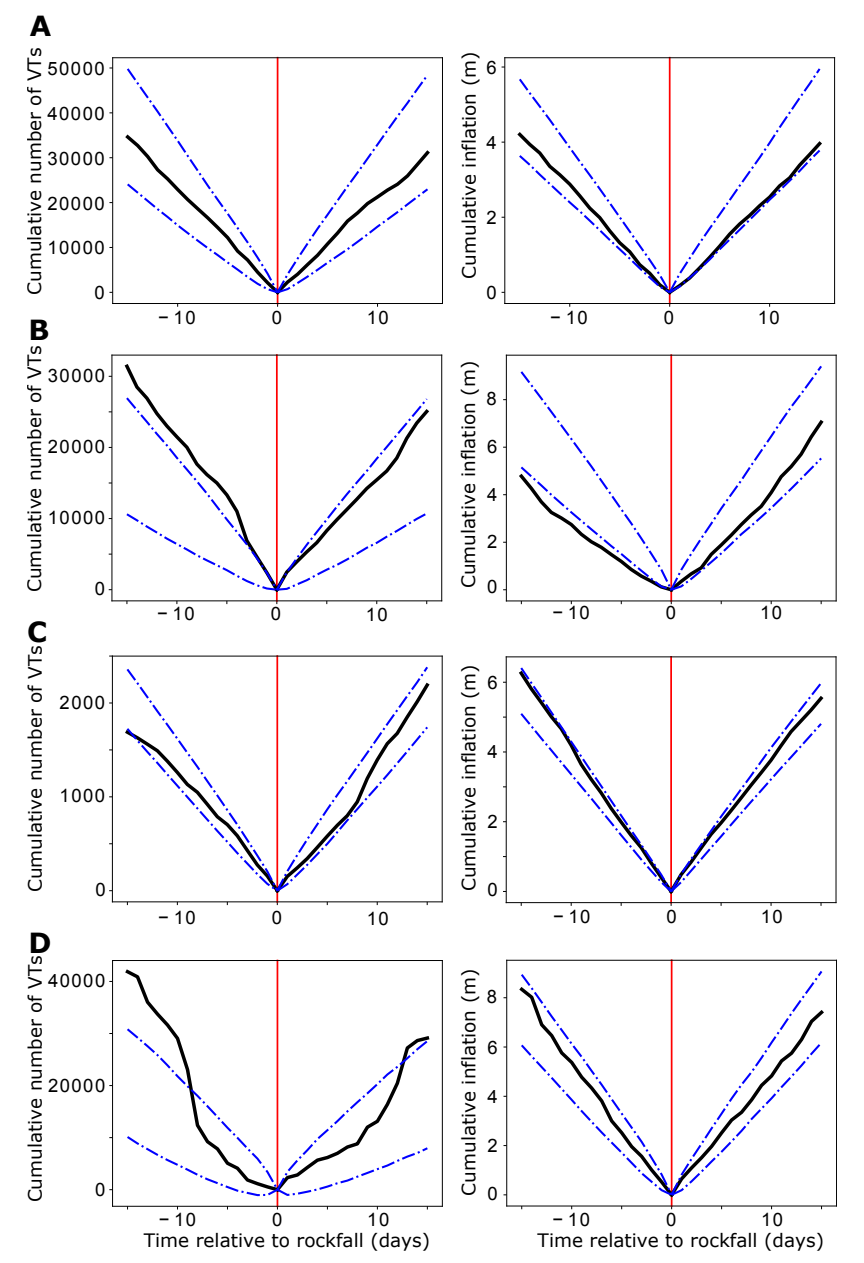


Supplementary Figure S9 Comparison of the rockfall background activity to the Seismic Moment of the volcano-tectonic events. (A) Seismic Moment of volcano-tectonic events (VT, black) vs. the number of rockfalls (RF, red), both summed on 15 days. The vertical gray lines and rectangles show the start times and durations of eruptions. (B) to (E) Statistical significance of the effect of seismicity on rockfall triggering. The plots are centered on the rockfall occurrence (red vertical line). The black lines represent the stacked seismicity data for each rockfall. The periods used for each plot are indicated on Fig.4A in the main text.

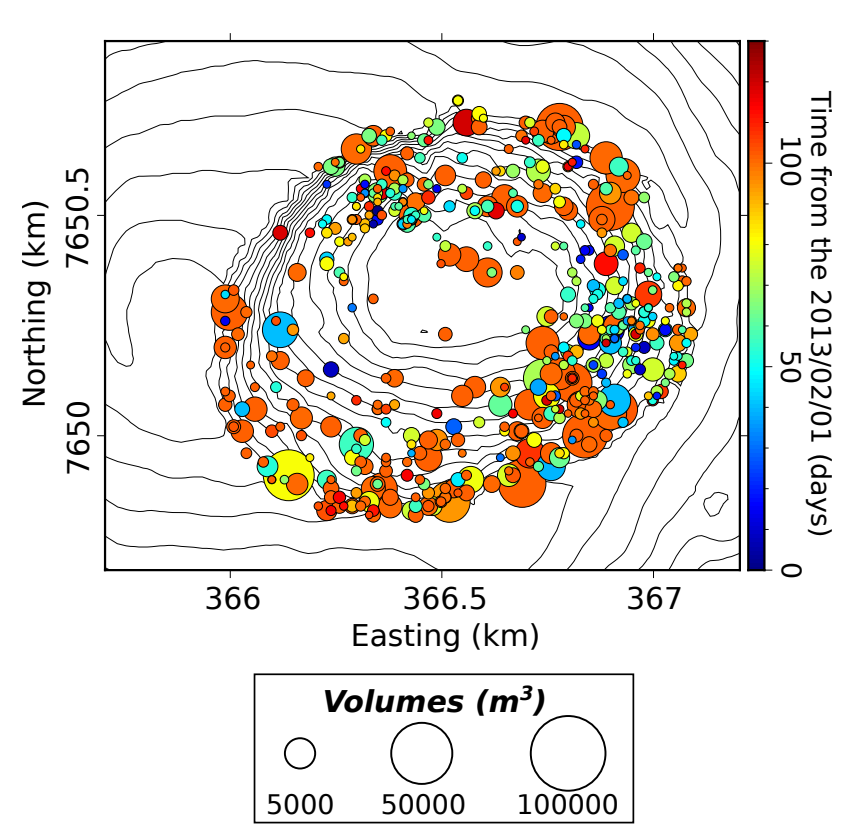


Supplementary Figure S10 Comparison of the temporal evolution of the rockfalls and of the deflation and inflation of the volcano cone. On the 10 years period, periods of inflation and deflation alternate. Here, we separate the periods of inflation (positive slope) and the periods of deflation (negative slope) to highlight their potential effect on rockfall triggering. The deflation rate is mostly constant over time, and is therefore less likely to trigger rockfall activity. The inflation rate shows more variations, that may be correlated with increases of rockfall activity. The upper panel shows the temporal evolution of all the rockfalls (V;100 m3), the bottom panel shows the temporal evolution of the deflation and the inflation of the cone using two different baselines. The vertical gray lines and rectangles show the start times and duration of eruptions.

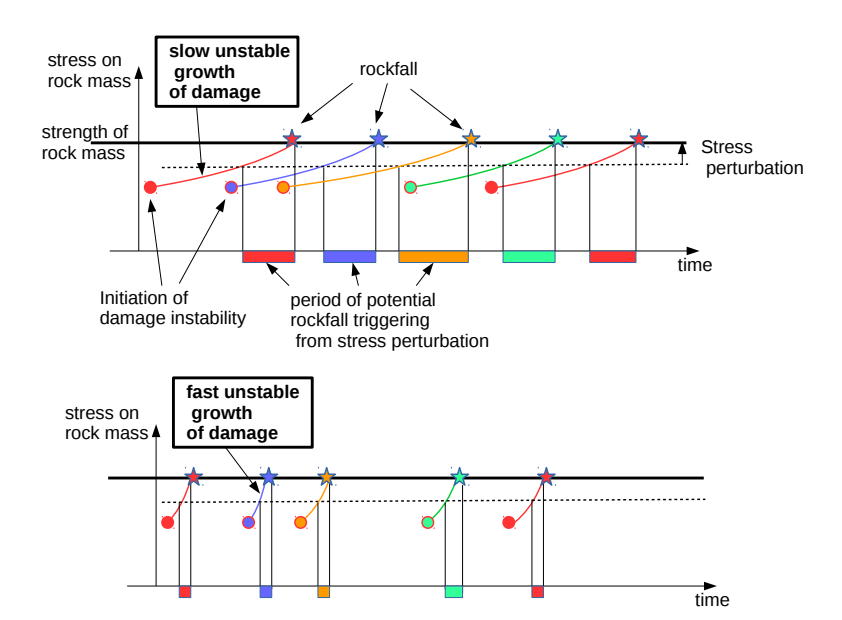
## 14 Article Title



Supplementary Figure S11 Statistical tests to differentiate the impact of seismicity (VTs) and deformation on rockfall triggering. For the deformation, we consider here only the inflation component, which is the larger than the deflation component (see Fig. S2). Left column: Statistical significance of the effect of seismicity on rockfall triggering when seismicity is dominant (the number of events per day being larger than the seismicity median, along with the deformation rate being smaller than the deformation rate median). Right column: Statistical significance of the effect of deformation on rockfall triggering when inflation rate is dominant (the deformation rate per day being larger than the deformation median, along with the seismic activity being smaller than the seismicity median). (A) Period 1. (B) Period 2. (C) Period 3. (D) Period 4. The periods used for each plot are indicated on Fig. 3A and 4 in the main text.



Supplementary Figure S12 Spatio-temporal evolution of the rockfalls during the 2013 crisis (2013/02/01-2013/06/13). The size of the circles scales with the volumes of the rockfalls, the colors represent the time from 2013/02/01.



Supplementary Figure S13 Schematic representation of the different mechanisms driving rockfalls during Periods 1 and 2. (A) This sketch represents the rapid growth of damage and fracture during Period 1, when the crater walls are more unstable, due to the relaxation following the crater floor collapse. This rapid growth leads to a very short "effective" time window (colored rectangles along the time line) during which the stress perturbations generated by the external forcings can interact with the damage growth. (B) On the contrary, this sketch represents the slow growth of damage and fracture during Period 2, when the crater walls are more stable. This slow growth leads to a long "effective" time window (colored rectangles along the time line) during which the stress perturbations generated by the external forcings can interact with the damage growth and advance the final rupture time. There is therefore more probability during this stable period that low level perturbations from seismicity and rain may find many mature rock masses with  $\tau_0$  close to the threshold, and thus may trigger their advanced failure, and statistically outnumber the slowly self-rising ruptures.